Permafrost carbon as a missing link to explain CO$_2$ changes during the last deglaciation

K. A. Crichton[1,2]*[†], N. Bouttes[3], D. M. Roche[4,5], J. Chappellaz[1,2] and G. Krinner[1,2]

The atmospheric concentration of CO$_2$ increased from 190 to 280 ppm between the last glacial maximum 21,000 years ago and the pre-industrial era[1,2]. This CO$_2$ rise and its timing have been linked to changes in the Earth's orbit, ice sheet configuration and volume, and ocean carbon storage[2,3]. The ice-core record of $\delta^{13}CO_2$ (refs 2,4) in the atmosphere can help to constrain the source of carbon, but previous modelling studies have failed to capture the evolution of $\delta^{13}CO_2$ over this period[5]. Here we show that simulations of the last deglaciation that include a permafrost carbon component can reproduce the ice core records between 21,000 and 10,000 years ago. We suggest that thawing permafrost, due to increasing summer insolation in the northern hemisphere, is the main source of CO$_2$ rise between 17,500 and 15,000 years ago, a period sometimes referred to as the Mystery Interval[6]. Together with a fresh water release into the North Atlantic, much of the CO$_2$ variability associated with the Bølling–Allerod/Younger Dryas period ~15,000 to ~12,000 years ago can also be explained. In simulations of future warming we find that the permafrost carbon feedback increases global mean temperature by 10–40% relative to simulations without this feedback, with the magnitude of the increase dependent on the evolution of anthropogenic carbon emissions.

We approach the problem of constraining the response of the permafrost-carbon pool to changing climate by studying the past, and specifically using the ice core record of the ratio of ^{13}C to ^{12}C in the atmosphere. The ratio, described by its $\delta^{13}CO_2$ value[7], is strongly affected by the exchange of carbon between the biosphere and the atmosphere because photosynthesis preferentially takes up ^{12}C, resulting in a low $\delta^{13}CO_2$ in biosphere-derived carbon, at a mean value around $-25‰$ (ref. 8).

The ice core record for $\delta^{13}CO_2$ for the last glacial termination shows a fast drop of ~0.4‰ occurring between 17.5 kyr to 16 kyr BP (refs 2,4) (BP is before present) at the same time as a rise of ~35 ppm in CO$_2$ (ref. 1). This strongly suggests a biosphere-derived carbon source. Studies aiming to determine the source of the CO$_2$ rise point towards the deep Southern Ocean, where changes in ocean $\delta^{13}C$ indicate a release of ^{13}C-depleted carbon[2,3]. However, modelling studies simulating changes in ocean circulation have not been able to explain the full change seen in the atmospheric $\delta^{13}CO_2$ record. A previous study[9] indicates that the terrestrial biosphere (including living plants and dead organic matter in all soils) grew by a total of 330 GtC between the Last Glacial Maximum (LGM) and the present day, but also indicates that a loss of 700 GtC was seen in the inert carbon pool. Here we consider the inert carbon pool to be

the permafrost-carbon pool[10,11], which at present holds an estimated 1,000 to 1,500 GtC (ref. 12).

We propose that, during the glacial termination, orbital changes that increased summer insolation in the northern high and mid-latitudes resulted in much carbon being released to the atmosphere from thawing permafrost soils, and that may provide an explanation for the changes seen in the CO$_2$ and $\delta^{13}CO_2$ record at the onset of deglaciation.

We have implemented a simplified permafrost-carbon mechanism[13] into the Earth System Model of Intermediate Complexity (EMIC), CLIMBER-2[5,14–16]. The CLIMBER-2 model includes modules simulating the atmosphere, ocean and terrestrial biosphere. It simulates the carbon cycle fluxes between these three components, including a biogeochemical model in the ocean[16,17]. CLIMBER-2 also accounts for glacial ocean mechanisms[5,18], principally the sinking of brines to the deep ocean as a result of sea ice formation, which result in a deep Southern Ocean carbon pool at LGM that is then released during deglaciation, as suggested by deep ocean data[2,19]. We build on a previous study using these glacial ocean mechanisms[5], and add our new permafrost-carbon mechanism (see Methods and ref. 13) for the terrestrial biosphere. Our model is the first that includes a palaeo-data validated dynamic representation of a permafrost-carbon pool for the last deglaciation.

We ran three experiments with our coupled model. OLA (Ocean Land Atmosphere) with glacial ocean mechanisms; POLA (Permafrost Ocean Land Atmosphere), where permafrost carbon is added; POLA$_{FWF}$ (with fresh water forcing added), where fresh water is released into the North Atlantic during the deglaciation. Model drivers and settings are in Fig. 1 (see Methods).

The OLA experiment simulates the 100 ppm rise in CO$_2$ observed in data between the LGM and the pre-industrial period (Fig. 2a), which has also been seen in previous studies[3,5]. The timing of the model CO$_2$ rise is largely determined by the rate of the release of the Southern Ocean carbon pool, due to the change in Southern Ocean stratification. This is governed by the sinking brines (Fig. 1b) and is fully described in a previous study[5,18]. It is linked to the interaction between the Antarctic ice sheet and sea-level changes. This mechanism alone, however, cannot explain the evolution of the $\delta^{13}CO_2$ data[5].

In POLA, permafrost extent, calculated using Frost Index[13] responds to changes in seasonal patterns of insolation caused by changes in orbit. The increase in summer insolation (Fig. 1a), and climate feedbacks, in northern high and mid-latitudes occurring between 24 kyr to 11 kyr BP causes a reduction in permafrost extent and a release of carbon from those thawed soils. This plant-based

[1]CNRS, LGGE (UMR5183), F-38041 Grenoble, France. [2]Univ. Grenoble Alpes, LGGE (UMR5183), F-38041 Grenoble, France. [3]UMR CNRS 5805 EPOC – OASU, Université de Bordeaux, 33615 PESSAC CEDEX, France. [4]Laboratoire des Sciences du Climat et de l'Environnement, LSCE/IPSL, CEA-CNRS-UVSQ, Université Paris-Saclay, F-91191 Gif-sur-Yvette, France. [5]Cluster Earth and Climate, Department of Earth Sciences Faculty of Earth and Life Sciences, Vrije Universiteit Amsterdam De Boelelaan 1085, 1081 HV Amsterdam, The Netherlands. [†]Present address: School of Earth and Ocean Sciences, Cardiff University, Park Place, Cardiff CF10 3AT, UK. *e-mail: CrichtonK@cardiff.ac.uk
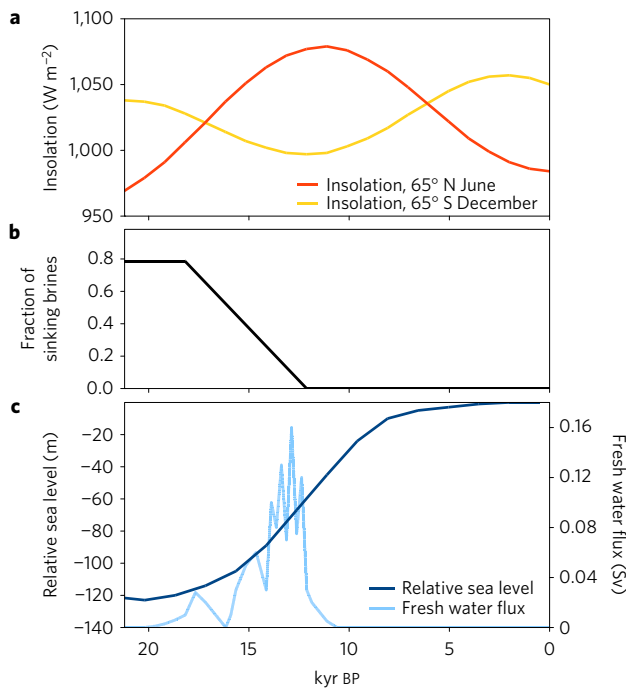
Figure 1 | Model drivers and settings for the deglaciation simulations.
a, Changes in insolation at 65° N in June and 65° S in December due to orbital changes (red and orange, respectively)[27]. **b**, Evolution of the parameter controlling the sinking of salty waters due to sea ice formation (brines) to the deep ocean, resulting in vertical stratification[5] (grey).
c, Model relative sea level controlling land ice extent; ocean salinity and nutrients concentrations (dark blue) (based on ref. 28), and the fresh water flux for the North Atlantic used in the POLA$_{FWF}$ simulation (light blue).

carbon, with low δ^{13}C, produces a drop in atmospheric $\delta^{13}CO_2$ (seen in Fig. 2b, see also Supplementary Discussion A–C). The dynamics (retreat) of the ice sheet over land also play a strong role in determining total permafrost surface area. In the POLA simulation the ocean is a net carbon sink from 17.5 kyr to ~15 kyr BP and permafrost-derived carbon drives the increase in atmospheric CO_2. During the same period, the active land carbon pool (vegetation and near-surface soils) is increasing, as plants globally respond to more favourable growing conditions as temperatures rise. After 14 kyr BP the land becomes a net carbon sink and the increase in atmospheric CO_2 is from the ocean.

Between 14 kyr and 12 kyr BP, the CO_2 plateau seen in ice core data is not reproduced in either the OLA or POLA simulations. Studies suggest that this CO_2 plateau, and coincident Northern Hemisphere cooling, may have been a result of the collapse of the Atlantic Meridional Overturning Circulation (AMOC)[20,21], possibly via ice melt into the Atlantic. Using an iterative trial and improvement method driven only by the fit to the CO_2 record[1], we arrived at an evolving fresh water flux with a modelled CO_2 output in POLA$_{FWF}$ that shows a good match with data between 20 kyr to 10 kyr BP. The modelled $\delta^{13}CO_2$ in the POLA$_{FWF}$ simulation also shows a better fit to mean data than POLA for the timing of the drop at ~17.5 kyr BP (see Supplementary Discussion D for more on $\delta^{13}CO_2$ and POLA$_{FWF}$). The fresh water flux that we derived from the iterative method (shown in Fig. 1c) is in broad agreement with the sea-level record, with the strongest flux coinciding with the timing of MWP1a (ref. 22), around 14 kyr BP.

The fresh water forcing not only results in model–data agreement with the CO_2 record, but also results in better agreement between model and data temperature anomalies in the Northern Hemisphere (Fig. 2c). Modelled Northern Hemisphere warming in the period
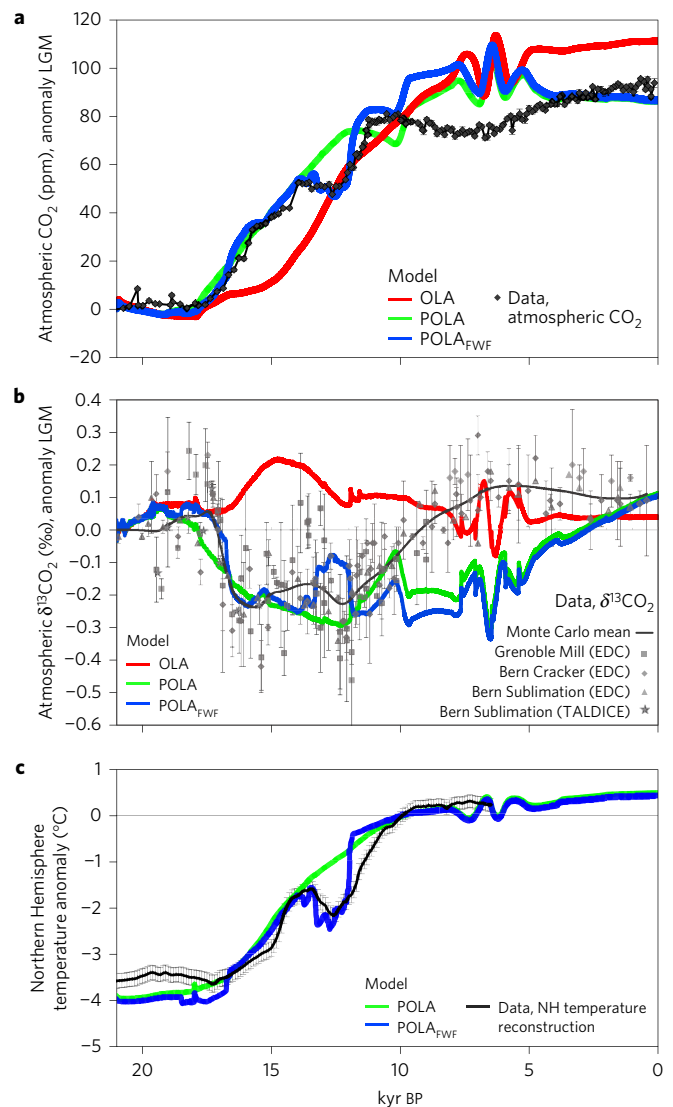
Figure 2 | Evolution of atmospheric CO_2, $\delta^{13}CO_2$ and Northern Hemisphere temperature in model and data. a, Atmospheric CO_2 concentration anomaly from LGM in ppm for three model outputs and data[1], **b**, Atmospheric $\delta^{13}CO_2$ for three model outputs and data[4].
c, Reconstructed Northern Hemisphere temperature anomaly[29] with model output overlaid. OLA is the CLIMBER-2 standard model and glacial ocean mechanisms. POLA is OLA plus the permafrost-carbon mechanism, POLA$_{FWF}$ is POLA plus a fresh water flux shown in Fig. 1 applied in the North Atlantic. For figure **c** OLA (not shown) has the same temperature profile as POLA.

12.5 to 11.5 kyr BP is faster than data, but the model rate of CO_2 rise is also faster than data, so this tends to support our hypothesis.

We compare model ocean δ^{13}C with ocean data for two ocean regions (Fig. 3). Model output is in the range of deep ocean δ^{13}C data uncertainty in the deep Southern Ocean, where the glacial carbon stock is progressively released during the deglaciation. For the surface North Atlantic waters, POLA and POLA$_{FWF}$ show better agreement with data than OLA between 21 kyr BP and ~15 kyr BP as the data δ^{13}C decreases. This region of ocean water is a carbon sink for atmospheric carbon at this time; the fall in atmospheric $\delta^{13}CO_2$ is reflected in the water δ^{13}C signature. The oceanic δ^{13}C is also affected by changes in circulation. We limited the North Atlantic data to the West Atlantic current, (which is more representative of our basin-averaged ocean model). This could partially explain the mismatch after 15 kyr BP, when the model outputs are at the lower
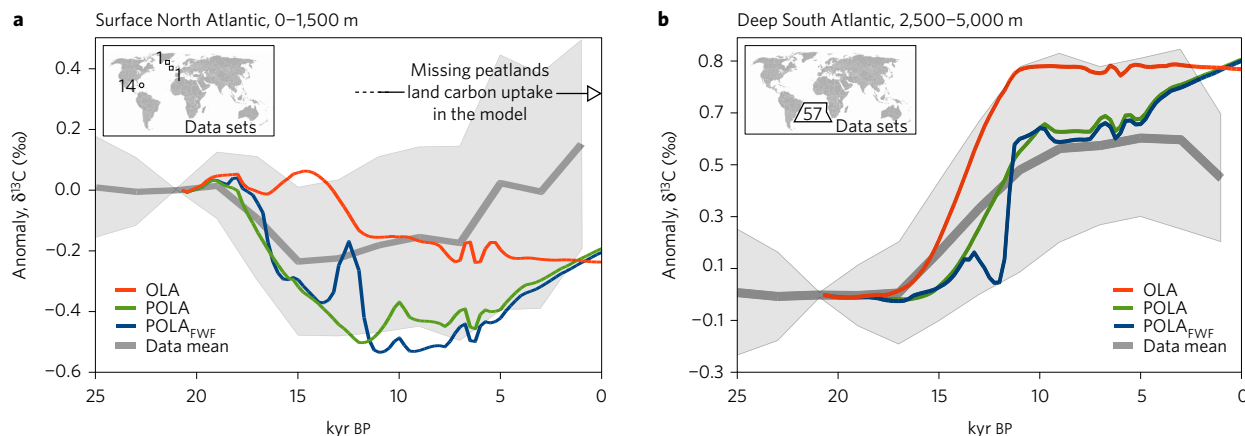
Figure 3 | Evolution of ocean δ13C in model and data. a,b, Data[19] are for benthic δ13C with one standard deviation data range (grey shading). Model output is for matching depth and latitude bands as data. The number of data sets and their locations are indicated on the maps. Missing peatlands expansion period shown. **a**, Surface North Atlantic waters (data only for the western current). **b**, Deep South Atlantic waters.

end of data uncertainty (see Supplementary Discussion E). When the fresh water flux is added in POLA$_{FWF}$, model output is still largely within the 1σ error of the data[19].

After around 10 kyr BP our model (POLA and POLA$_{FWF}$) diverges from data for both CO_2 and $\delta^{13}CO_2$. We attribute this to a missing land carbon sink, peatlands, which since 11 kyr BP have accumulated an estimated up to 500 GtC (ref. 23) but are not included in our model. Divergence may also be due to shallow water sedimentation[24] of $CaCO_3$, which we do not model. A terrestrial uptake (in peatlands) of 500 GtC would shift atmospheric $\delta^{13}CO_2$ by over 0.25‰ and CO_2 by more than 10 ppm at equilibrium (according to previous simulations). In CLIMBER-2, at a mean rate of 0.04 GtC yr^{-1} accumulation[23], system equilibration would take longer than the 10 kyr of the Holocene, so we expect shifts in $\delta^{13}CO_2$ and CO_2 to be higher in the shorter term.

A strong perturbation is seen in model output between 7 kyr to 5 kyr BP. This is due to high instability and then final collapse of model vegetation in the Sahara/Sahel region, caused by orbital changes[25].

In the Holocene period (from ∼8 kyr BP), the POLA and POLA$_{FWF}$ simulations show a gradual fall in CO_2 which is a result of continuing land carbon uptake in permafrost soils (due to slow accumulation rates). Data for CO_2 and $\delta^{13}CO_2$ indicate rather a slight fall in land carbon stocks from ∼8 kyr BP. We do not model anthropogenic land-use change or fire emissions[26], which may explain this discrepancy. By the present day, our modelled total land carbon stock is 4,425 GtC, compared to 3,970 ± 325 GtC from the data estimate[9].

Our model is a simplified representation of the Earth system. We do not model changes in coastlines, so do not consider the flooding of continental shelves (see Supplementary Discussion F), which may have had a role to play in the carbon cycle during the glacial termination, although this is not well constrained.

We carried out a series of future projections using our palaeo-data validated model. We found that projected carbon losses from permafrost thaw were in agreement with other up-to-date studies (see Supplementary Discussions G, H and I). From 2010 to 2100 we project losses of 42 GtC to 45 GtC for Representative Emission Pathways (REPs) 2.6, 4.5 and 6.0 and 77 GtC loss for REP 8.5. By 2200 these range from 67 GtC for REP 2.6 and 389 GtC for REP 8.5. Our control simulation, without anthropogenic emissions, showed an uptake of carbon in permafrost soils, a slow increase in permafrost area, and a global cooling driven by climate feedbacks via the carbon cycle. With the benefit of a fully coupled future simulation (where carbon losses from thawing permafrost also contribute to temperature rise) we found that permafrost carbon increased

peak global temperatures by 10–40% compared to model output that did not include it, with REP 4.5 the most affected. The timing of peak temperature depends on the REP. The future role of the large carbon stock in peatland/wetland soils, identified as a source of model–data mismatch during the Holocene, is currently not well constrained (whether a positive or negative feedback) in other studies.

We propose that permafrost plays a major role in the carbon cycle, especially during fast warming events affecting high latitudes. For the deglaciation period, permafrost carbon, when combined with the Glacial Southern Ocean's gradual carbon release, provides a plausible explanation for the evolution of $\delta^{13}CO_2$ and CO_2 seen in data, and this also affects ocean $\delta^{13}C$ values. How important the release of permafrost carbon is in magnifying the orbital forcing to trigger deglaciation is an open question. The permafrost-carbon dynamic also provides a plausible link for the changes seen in the temperature record and CO_2 record during the Bølling–Allerød and Younger Dryas period.

Methods

Methods, including statements of data availability and any associated accession codes and references, are available in the online version of this paper.

References

1. Lüthi, D. *et al*. EPICA Dome C Ice Core 800 KYr Carbon Dioxide Data. IGBP PAGES/World Data Center for Paleoclimatology Data Contribution Series # 2008–055. NOAA/NCDC Paleoclimatology Program (2008).
2. Lourantou, A. *et al*. Constraint of the CO_2 rise by new atmospheric carbon isotopic measurements during the last deglaciation. *Glob. Biogeochem. Cycles* **24**, GB2015 (2010).
3. Sigman, D. M., Hain, M. & Haug, G. H. The polar ocean and glacial cycles in atmospheric CO_2 concentration. *Nature* **446**, 47–55 (2010).
4. Schmitt, J. *et al*. Carbon isotope constraints on the deglacial CO_2 rise from ice cores. *Science* **336**, 711–714 (2012).
5. Bouttes, N. *et al*. Impact of oceanic processes on the carbon cycle during the last termination. *Clim. Past* **8**, 149–202 (2012).
6. Denton, G. H., Broecker, W. S. & Alley, R. B. The mystery interval 17.5 to 14.5 kyrs ago. *PAGES News* **14**, 14–16 (2006).
7. Craig, H. Isotopic standards for carbon and oxygen and correction factors for mass-spectrometric analysis of carbon dioxide. *Geochim. Cosmochim. Acta* **12**, 133–149 (1957).
8. Maslin, M. A. & Thomas, E. Balancing the deglacial global carbon budget: the hydrate factor. *Quat. Sci. Rev.* **22**, 1729–1736 (2003).
9. Ciais, P. *et al*. Large inert carbon pool in the terrestrial biosphere during the Last Glacial Maximum. *Nat. Geosci.* **5**, 74–79 (2012).

10. Zech, R., Huang, Y., Zech, M., Tarozo, R. & Zech, W. High carbon sequestration in Siberian permafrost loess-paleosols during glacials. *Clim. Past* **7,** 501–509 (2011).

11. Zimov, N. S. *et al*. Carbon storage in permafrost and soils of the mammoth tundra-steppe biome: role in the global carbon budget. *Geophys. Res. Lett.* **36,** L02502 (2009).

12. Hugelius, G. *et al*. Estimated stocks of circumpolar permafrost carbon with quantified uncertainty ranges and identified data gaps. *Biogeosciences* **11,** 6573–6593 (2014).

13. Crichton, K. A., Roche, D. M., Krinner, G. & Chappellaz, J. A simplified permafrost-carbon model for long-term climate studies with the CLIMBER-2 coupled Earth system model. *Geosci. Model Dev.* **7,** 3111–3134 (2014).

14. Petoukhov, V. *et al*. CLIMBER-2: a climate system model of intermediate complexity. Part 1: model description and performance for present climate. *Clim. Dynam.* **16,** 1–17 (2000).

15. Ganopolski, A. *et al*. CLIMBER-2: a climate system model of intermediate complexity. Part II: model sensitivity. *Clim. Dynam.* **17,** 735–751 (2001).

16. Brovkin, V., Ganopolski, A., Archer, D. & Rahmstorf, S. Lowering of glacial atmospheric CO_2 in response to changes in oceanic circulation and marine biogeochemistry. *Paleoceanography* **22,** PA4202 (2007).

17. Brovkin, V., Hofmann, M., Bendtsen, J. & Ganopolski, A. Ocean biology could control atmospheric $\delta^{13}C$ during glacial-interglacial cycle. *Geochem. Geophys. Geosyst.* **3,** 1–15 (2002).

18. Bouttes, N., Paillard, D., Roche, D. M., Brovkin, V. & Bopp, L. Last glacial maximum CO_2 and $\delta^{13}C$ succesfully reconciled. *Geophys. Res. Lett.* **38,** L02705 (2011).

19. Oliver, K. I. C. *et al*. A synthesis of marine sediment core ^{13}C data over the last 150 000 years. *Clim. Past* **6,** 645–673 (2010).

20. Kageyama, M., Paul, A., Roche, D. M. & Van Meerbeeck, C. J. Modelling glacial climatic millennial-scale variability related to changes in the Atlantic Meridional Overturning Circulation: a review. *Quat. Sci. Rev.* **29,** 2931–2956 (2010).

21. Tarasov, L. & Peltier, W. R. Arctic freshwater forcing of the Younger Dryas cold reversal. *Nature* **435,** 662–665 (2005).

22. Lambeck, K., Rouby, H., Purcell, A., Sun, Y. & Sambridge, M. Sea level and global ice volumes from the Last Glacial Maximum to the Holocene. *Proc. Natl Acad. Sci. USA* **111,** 15296–15303 (2014).

23. Yu, Z., Loisel, J., Brosseau, D. P., Beilman, D. W. & Hunt, S. J. Global peatland dynamics since the Last Glacial Maximum. *Geophys. Res. Lett.* **37,** L12402 (2010).

24. Kleinen, T., Brovkin, V., von Bloh, W., Archer, D. & Munhoven, G. Holocene carbon cycle dynamics. *Geophys. Res. Lett.* **37,** L02705 (2010).

25. Brovkin, V. *et al*. Carbon cycle, vegetation, and climate dynamics in the Holocene: experiments with the CLIMBER-2 model. *Glob. Biogeochem. Cycles* **16,** 1139 (2002).

26. Ruddiman, W. F., Kutzbach, J. E. & Vavrus, S. J. Can natural or anthropogenic explanations of late-Holocene CO_2 and CH_4 increases be falsified? *Holocene* http://dx.doi.org/10.1177/0959683610387172 (2011).

27. Berger, A. Long-term variations of daily insolation and Quaternary climatic changes. *J. Atmos. Sci.* **35,** 2362–2367 (1978).

28. Waelbroeck, C. *et al*. Sea-level and deep water temperature changes derived from benthic foraminifera isotopic records. *Quat. Sci. Rev.* **21,** 295–305 (2002).

29. Shakun, J. D. *et al*. Global warming preceded by increasing carbon dioxide concentrations during the last deglaciation. *Nature* **484,** 49–54 (2012).

Author contributions

K.A.C. carried out the study and interpreted data, building on work from N.B. and D.M.R. for the deglaciation period, K.A.C. designed the fresh water forcing experiments. All authors contributed to writing the paper.

Additional information

Supplementary information is available in the online version of the paper. Reprints and permissions information is available online at www.nature.com/reprints. Correspondence and requests for materials should be addressed to K.A.C.

Competing financial interests

The authors declare no competing financial interests.

Methods

The permafrost-carbon mechanism is fully described and validated in a previous study[13]. As a summary, it identifies the fraction of a grid cell that is permafrost affected via a Frost Index calculation (the measure of the number of cold versus warm days in a year, this includes a snow correction). A fraction of the soil carbon, matching the permafrost fraction, in the grid cell experiences a reduced decay rate (compared to a standard grid cell). The permafrost fraction and carbon fluxes are calculated once a year.

Each simulation starts from an equilibrium glacial maximum climate (21 kyr BP, the LGM) where modelled CO_2 and Atlantic vertical $\delta^{13}C$ gradient agree with data[18,30] (see Supplementary Discussion A). The parameters for the ocean are chosen to best match the LGM data for atmospheric CO_2 and the vertical gradient of $\delta^{13}C$ in the Atlantic, similar to a previous study[30]. All simulations include a representation of the ocean carbon cycle including marine biota[16] and carbonate compensation[17]; dynamic vegetation; evolving Northern Hemisphere ice sheets driven by the sea-level record; orbital changes; an evolving deep Southern Ocean carbon pool due to the stratification in the Southern Ocean resulting from the sinking of salty waters rejected on sea ice formation (brines)[5,18]. All these are incorporated in the first experiment (OLA – Ocean Land Atmosphere), which is our standard deglacial simulation without permafrost and has been described in more detail in a previous study[5]. In the second experiment (POLA – Permafrost Ocean Land Atmosphere) the permafrost model is added. In a third experiment, a fresh water flux in the North Atlantic is prescribed (POLA_FWF). Drivers and settings for the model outputs are shown in Fig. 1.

The deglaciation simulations (glacial termination) have similar forcings to a previous study[5,18]. They are forced with CO_2 concentration data from 21 kyr BP to pre-industrial present for the radiative code of the model (without anthropogenic emissions). The ice sheets in the Northern Hemisphere evolve with land ice volume and extent determined by the sea-level record[5]. The salinity and nutrient concentration in the ocean are also evolving following the sea-level record, and insolation is computed from orbital changes. The parameter for the sinking of salty water from sea ice formation (brines) is reduced from its maximum value to zero linearly between 18 kyr and 12 kyr BP. The timing of the CO_2 rise seen in our model output for the OLA simulation is largely determined by the rate of the release of the Southern Ocean carbon pool due to the change in Southern Ocean stratification. This is governed by the parameter setting the fraction of salty water (brines) sinking to the deep ocean. In our simulation the evolution of the sinking salty water is conceptually driven by the interaction of the Antarctic ice sheet with the ocean. At low sea level and large extent of ice sheets, the salty waters do not mix easily with surrounding waters, and so sink efficiently. This efficiency decreases when sea level rises, more of the salty water is then mixed in the upper ocean and less reaches the abyss[5].

The dynamic response of the permafrost-carbon pool is studied by performing a series of experiments with permafrost-carbon settings that vary the dynamic response of carbon in these soils. This is fully described in a previous study[13]. For each simulation including permafrost-carbon, each dynamic setting is applied individually, resulting in four model outputs. The model setting shown in the main text is for the simulation where the model best fits the data for CO_2—in this case, the 'medium' permafrost-carbon dynamic setting. Model outputs for all POLA simulations are available in Supplementary Discussion A. The modelled CO_2 that we compare to data is computed by the carbon cycle model (whereas the radiative code is driven by data CO_2) for the palaeo simulations.

For the future projections, the simulations start from the deglaciation simulation for 'best fit' (medium permafrost dynamic) for the year 1850 (or 100 yr BP). In this set the radiative model and carbon cycle model are now fully coupled, so the carbon cycle calculated CO_2 concentration drives the radiative model. This allows us to drive the model with carbon emissions to the atmosphere (not imposed CO_2 concentrations) according to the REP emissions pathways for fossil fuel carbon emissions and land-use change. We use the extended emission pathway profiles, and further extend them. For REPs 2.6, 4.5 and 6 we reduce emissions linearly from 2100 to zero at 2200. For REP 8.5 we hold emissions fixed between 2100 to 2200 then reduce linearly to zero at 2300. Model output does not include any glacial ocean mechanisms. A compensation for the model's overestimate of Siberian carbon stocks[13] is done by removing 100% of the overestimate of carbon lost from these grid cells from the projections, in this case the model output being 2.5 times the data estimate for the top 1 m of soil (see Supplementary Discussion H). The compensation for global temperature output is done by linearly reducing the modelled temperature anomaly in proportion to the ratio of the corrected permafrost-carbon projection to the uncorrected projection. Therefore, for this adjustment we assume the permafrost-carbon feedback to be linear (within each REP).

Code availability. The code for the permafrost-carbon model used within CLIMBER-2 that generated the model results can be accessed at http://www.geosci-model-dev.net/7/3111/2014/gmd-7-3111-2014.html.

Data availability. The authors declare that the data supporting the findings of this study are available within the article and its Supplementary Information files.

References

30. Curry, W. B. & Oppo, D. W. Glacial water mass geometry and the distribution of $\delta^{13}C$ of ΣCO_2 in the western Atlantic Ocean. *Paleoceanography* **20,** PA1017 (2005).